

Hydrogen Bonding of Methyl Alcohol-*d* in Supercritical Carbon Dioxide and Supercritical Ethane Solutions

John L. Fulton, Geary G. Yee, and Richard D. Smith*

Contribution from the Chemical Methods and Separations Group, Chemical Sciences Department, Pacific Northwest Laboratory,[†] Richland, Washington 99352.

Received April 8, 1991

Abstract: Fourier transform infrared (FTIR) spectroscopy has been used to measure the degree of intermolecular hydrogen bonding between solute molecules of methyl alcohol-*d* in supercritical carbon dioxide, supercritical ethane, and liquid heptane. In these fluids, an equilibrium is established between the free non-hydrogen-bonded monomer and the various hydrogen-bonded species of which the tetrameric species is believed to predominate. The fluid pressure, temperature, and the alcohol concentration significantly affect the equilibrium distribution of the monomer and oligomeric species. Both supercritical and subcritical binary solutions containing up to 0.07 mole fraction of methyl alcohol-*d* were examined under conditions ranging from 30 to 400 bar and 40 to 80 °C. The changes in the partial molar enthalpies and partial molar volumes of the alcohol upon hydrogen bonding are reported. These measurements, together with evidence from coupled rotational-vibrational bands, point to the formation of some type of weak complex between carbon dioxide and methyl alcohol. Such a complex is likely the result of the interaction of the large carbon dioxide quadrupole with the methyl alcohol dipole. The solvation phenomena presented in this paper will provide for more complete thermodynamic treatments of these systems.

Introduction

An important and interesting class of binary solvent systems is one containing a small amount of a hydrogen-bonding solvent in a nonpolar supercritical fluid. The classic and perhaps most widely studied example of this type of system is the CO₂/methyl alcohol system. Supercritical fluids such as CO₂, which have moderate critical temperatures, are nonpolar or very low polarity solvents. The addition of small amounts of polar "modifiers" can be used to greatly enhance the solubility of moderately polar species in the fluid.^{1,2} In addition to the improved solvent properties, these binary systems retain the favorable mass transport properties for which supercritical fluids are well known such as their high molecular diffusivities and low viscosities.

The understanding of solvation in the simplest, non-hydrogen-bonding, binary supercritical fluid solutions is evolving to one that involves a local "clustering"³⁻⁵ of solvent molecules about the solute molecule. These "clusters" are defined as the excess number of solvent molecules about the solute in excess of the bulk density and are different from gas-phase clusters formed upon the adiabatic expansion of a gas. This "clustering" phenomenon becomes very pronounced near the critical point of the solution where tens to hundreds of solvent molecules can be clustered around a single solute molecule. Such clustering causes local increases in fluid density that explicitly contradict the early models invoked for these systems. In addition to the solvent-solute "clustering" observed in dilute solutions, in more concentrated solutions the solutes can form clusters with other solute molecules.⁶ For solutes having high polarity, or high polarizabilities, such solute-solute "clusters" can form at surprisingly low concentrations.

The solvation behavior of these "simple" supercritical solutions can be contrasted with supercritical systems in which a solute or solvent modifier can form hydrogen bonds. In addition to the expected "clustering" of solvent molecules around the solute, there is a very different type of clustering equilibrium which exists for this type of system. Free, non-hydrogen-bonded solutes establish an equilibrium with aggregates of hydrogen-bonded solute clusters of various stoichiometric sizes. Spectroscopic studies of hydrogen bonding of alcohols in apolar liquid solvents extend back 50 years.⁷⁻⁹ Such studies have suggested that alcohol molecules form hydrogen-bonded "clusters" in apolar liquid solvents consisting of from two to six molecules per cluster. The extent of hydrogen bonding of alcohols in apolar liquid solvents is consistent with a simple mass-action-type of model. At low concentrations¹⁰ (mole fraction alcohol, $x_{\text{alcohol}} < 0.003$), the alcohol exists in the monomer

form. Upon increasing the concentration, the aggregation progresses through dimer, trimer, to tetramer and higher oligomers at high concentrations of the alcohol. Even after 50 years of spectroscopic studies, there is disagreement on the types of hydrogen-bonded species in such apolar liquid solvents. However, the existing evidence indicates that, although a multitude of hydrogen-bonded species exist in solution, there are two hydrogen-bonded species that appear to have special stability: the linear dimer and cyclic tetramer.⁹⁻¹¹

The various studies of alcohol hydrogen bonding in solids, liquids, and in the gas phase have been conducted from both experimental and theoretical points of view. In a recent study, Karachewski et al.¹² looked at hydrogen bonding of alcohols in apolar liquid solvents using NMR. Using a combined chemical-physical model which utilized the NMR data, they showed that at low mole fractions of the alcohol the tetrameric species was dominant. Information on structures of the various hydrogen-bonded species has been obtained from infrared matrix isolation studies^{13,14} and from IR photodissociation spectra of gas-phase clusters isolated in molecular beams.¹⁵ These studies clearly favor a linear dimer species rather than the cyclic structure. The trimer and higher oligomers are preferentially cyclic structures in the gas phase.¹⁵ The structure of various hydrogen-bonded methyl alcohol species has also been determined from ab initio molecular orbital calculations.^{16,17} This approach also favors the

(1) Dobbs, J. M.; Wong, J. M.; Lahiere, R. J.; Johnston, K. P. *Ind. Eng. Chem. Res.* **1987**, *26*, 56-65.

(2) Dobbs, J. M.; Johnston, K. P. *Ind. Eng. Chem. Res.* **1987**, *26*, 1476-1482.

(3) Brennecke, J. F.; Tomasko, D. L.; Peshkin, J.; Eckert, C. A. *Ind. Eng. Chem. Res.* **1990**, *29*, 1682-1690.

(4) Kim, S.; Johnston, K. P. *Ind. Eng. Chem. Res.* **1987**, *26*, 1206-1213.

(5) Yonker, C. R.; Smith, R. D. *J. Phys. Chem.* **1988**, *92*, 1664-1667.

(6) *Supercritical Fluid Science and Technology*; Johnston, K. P., Penninger, J. M. L., Eds.; ACS Symposium Series 406, American Chemical Society: Washington, DC, 1989.

(7) Badger, R. M.; Bauer, S. H. *J. Chem. Phys.* **1937**, *5*, 839-851.

(8) Van Ness, H. C.; Winkle, J. V.; Richtol, H. H.; Hollinger, H. B. *J. Phys. Chem.* **1967**, *71*, 1483-1494.

(9) Fletcher, A. N.; Heller, C. A. *J. Phys. Chem.* **1967**, *71*, 3742-3756.

(10) Aveyard, R.; Briscoe, B. J.; Chapman, J. *J. Chem. Soc., Faraday Trans. 1* **1973**, *69*, 1772-1778.

(11) Curtiss, L. A. *J. Chem. Phys.* **1977**, *67*, 1144-1149.

(12) Karachewski, A. M.; Howell, W. J.; Eckert, C. A. *AIChE J.* **1991**, *37*, 65-73.

(13) Murto, J.; Rasanen, M.; Aspiala, A.; Kemppinen, E. *Acta Chem. Scand. A* **1983**, *37*, 323-335.

(14) Schriver, L.; Burneau, A.; Perchard, J. P. *J. Chem. Phys.* **1982**, *77*, 4926-4932.

(15) Buck, U.; Gu, X.; Lauenstein, C.; Rudolph, A. *J. Phys. Chem.* **1988**, *92*, 5561-5562.

(16) Jorgensen, W. L. *J. Chem. Phys.* **1979**, *71*, 5034-5038.

* Corresponding author.

[†] Operated by Battelle Memorial Institute.

linear dimer over the cyclic one and likewise predicts that the higher oligomers are cyclic. An ab initio study by Curtiss showed that of the trimer and higher cyclic oligomers the cyclic tetramer had a special stability.¹¹

Because of the importance of modified supercritical fluids for separations, the phase behavior of simple alcohols in supercritical fluids has been the subject of numerous studies.^{18–20} Friedrich et al.²¹ used the near-infrared spectroscopic technique to examine the partitioning of C₆ and C₈ alcohols in supercritical carbon dioxide. Several authors have modeled the thermodynamics of these alcohol/fluid systems.^{4,22} However, these thermodynamic treatments have not directly addressed the presence of various hydrogen-bonded species in solution. Since the formation of hydrogen bonds in solution represents a type of chemical equilibrium, in this study we have chosen to describe the hydrogen bonding of methyl alcohol from a microscopic perspective. We expect that the chemical equilibrium between methyl alcohol monomers and hydrogen-bonded oligomers will be strongly affected by the density and temperature of the supercritical fluid. The novel effects of the density of the supercritical fluid on reaction equilibria, and of special effects near the critical point, have been well-described by Peck et al.²³

In this study we use Fourier transform infrared spectroscopy to determine the extent of hydrogen bonding of methyl alcohol in supercritical carbon dioxide and supercritical ethane. Infrared spectroscopy provides a window on solvation mechanisms in supercritical fluids which has been greatly under-utilized until recently. We expect FTIR spectroscopy to have particular utility for studies of supercritical fluid phenomena, including the measurement of vibrational and rotational-vibrational bands of solutes in supercritical fluids for the study of (i) solute partitioning,²⁴ (ii) chemical reactions in situ, (iii) solvation phenomena from frequency shifts and intensity changes of solutes,^{25,26} and (iv) secondary energy effects such as molecular rotation. Concerning the latter, small solute molecules such as water or ammonia are believed to have an appreciable amount of rotational freedom in liquid alkane solvents.²⁷ For supercritical fluid solvents the degree of rotational freedom will depend on fluid density. Small solute molecules such as water or methyl alcohol may have a large amount of rotational freedom in low-density supercritical fluid solutions. Chialvo et al.²⁸ studied the phenomenon of solute rotation in supercritical fluids by using molecular dynamics simulations to determine the rotational relaxation times of pure carbon dioxide at different fluid densities. IR spectroscopy is one technique which is suited for experimentally measuring rotation of solute and solvent molecules in solution and should provide information on the amount of rotational freedom.

We have previously reported aggregation numbers for dodecanol-*d* in CO₂ and ethane in the range of from 3 to 5.²⁹ This

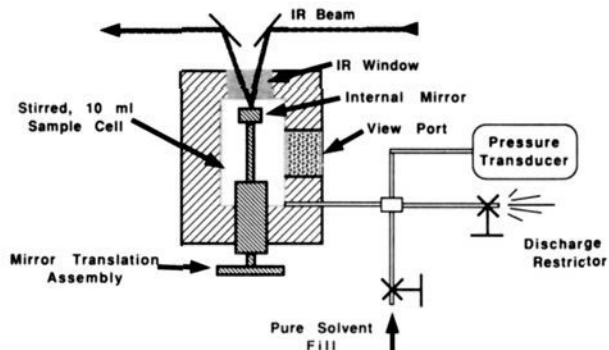


Figure 1. Schematic of the high-pressure IR cell and the associated solvent transfer lines.

study confirmed the expectation that the alcohol aggregation in supercritical fluids such as CO₂ is similar to that observed in liquid and gas phases. It appears that aggregation due to hydrogen-bonded cluster formation is generally similar in the gas, liquid, and supercritical fluid phases. Evidence of tetrameric methyl alcohol aggregates have been found in both the liquid³⁰ and the gas phases.³¹ In both phases, mixtures containing "low" concentrations of the alcohol contain only free monomer; higher concentration solutions contain progressively more tetrameric alcohol. Presumably the number or size of such clusters continues to increase up to the point of phase transition. Supercritical fluids allow one to vary the density from the gas- to the liquid-phase limits; therefore, measurements of hydrogen bonding in the gas and liquid phases provide approximate upper and lower bounds for cluster size and extent of hydrogen bonding to be found in supercritical fluids (except in the case of specific chemical interaction of the fluid with the aggregate).

In this study, we report the degree of intermolecular hydrogen bonding between solute molecules of methyl alcohol-*d* in three different solvents: carbon dioxide, ethane, and liquid heptane. The effects of the fluid pressure, temperature, and the alcohol concentration on the equilibrium distribution of the monomer and oligomeric species are determined. Both supercritical and subcritical binary solutions containing up to 0.07 mole fraction of methyl alcohol-*d* are examined under conditions ranging from 30 to 400 bar and 40 to 80 °C.

Experimental Section

The methyl alcohol-*d* with a reported purity of 99.5+ atom % deuterium and the nondeuterated anhydrous methyl alcohol with a purity of 99+% ("Gold Label") were used as received from Aldrich. "SFC Grade" carbon dioxide from Scott Specialty Gases had a reported purity of >99.98% and water content of <3 ppm (v/v). The ethane was "CP" grade from Alphagaz. Since trace amounts of water can significantly alter the aggregation of methyl alcohol molecules, both the ethane and the carbon dioxide were further dried by passing the saturated vapor through a large bed of molecular sieve. The anhydrous, 99% *n*-heptane (H₂O < 0.005%) was used as received from Aldrich.

A Nicolet 740 FT-IR spectrometer (Nicolet Analytical Instruments) purged with dry nitrogen was used to obtain all infrared spectra. The spectrometer was equipped with a germanium-on-KBr beam splitter and a mercury-cadmium-telluride detector. We co-added 128 scans at 4-cm⁻¹ wavenumber resolution to obtain the desired signal-to-noise ratio. The details of the design of the high-pressure cell and background subtraction technique are discussed in an earlier paper.²⁴ Briefly, the reflectance-type IR sample cell had a total volume of 10.0 mL. The contents could be stirred with a Teflon-coated, magnetically coupled stir bar. As shown in Figure 1, two optical windows were used: a single ZnSe window provided for transmission of both the incident and the reflected IR beam; a sapphire window provided for visual observation of the solution to determine the number of phases that were present. Because many of the systems in this study having higher mole fractions of the alcohol were subcritical,^{18,32} it is helpful to visually ensure that only one

(17) Damewood, J. R. Jr.; Kumpf, R. A.; Mühlbauer, W. C. F.; Urban, J. J. *J. Phys. Chem.* **1990**, *94*, 6619–6626.

(18) Robinson, D. B.; Peng, D.; Chung, S. Y. *Fluid Phase Equilibria* **1985**, *24*, 25–41.

(19) King, M. B.; Alderson, D. A.; Fallah, F. H.; Kassim, D. M.; Kassim, K. M.; Sheldon, J. R.; Mahmud, R. S. In *Chemical Engineering at Supercritical Fluid Conditions*; Paulitis, M. E., Penninger, J. M. L. J., Gray, R. D., Davidson, P., Eds.; Ann Arbor Science: Ann Arbor, MI, 1983; pp 31–80.

(20) McHugh, M. A.; Mallett, M. W.; Kohn, J. P. In *Chemical Engineering at Supercritical Fluid Conditions*; Paulitis, M. E., Penninger, J. M. L. J., Gray, R. D., Davidson, P., Eds.; Ann Arbor Science: Ann Arbor, MI, 1983; pp 113–137.

(21) Friedrich, J.; Schneider, G. M. *J. Chem. Thermodyn.* **1989**, *21*, 307–319.

(22) Christensen, J. J.; Cordray, D. R.; Oscarson, J. L.; Izatt, R. M. *J. Chem. Thermodyn.* **1988**, *20*, 867–875.

(23) Peck, D. G.; Mehta, A. J.; Johnston, K. P. *J. Phys. Chem.* **1989**, *93*, 4297–4304.

(24) Yee, G. G.; Fulton, J. L.; Blitz, J. P.; Smith, R. D. *J. Phys. Chem.* **1991**, *95*, 1403–1409.

(25) Luck, W. A.; Zheng, H. Y. *J. Chem. Soc., Faraday Trans. 2* **1984**, *80*, 1253–1268.

(26) Smith, R. D.; Fulton, J. L.; Blitz, J. P.; Tingey, J. M. *J. Phys. Chem.* **1990**, *94*, 781–787.

(27) Conrad, M. P.; Strauss, H. L. *J. Phys. Chem.* **1987**, *91*, 1668–1673.

(28) Chialvo, A. A.; Heath, D. L.; Debenedetti, P. G. *J. Chem. Phys.* **1989**, *91*, 7818–7830.

(29) Yee, G. G.; Fulton, J. L.; Smith, R. D. *Langmuir*, in press.

(30) Symons, M. C. R.; Thomas, V. J. *Chem. Soc., Faraday Trans. 1* **1981**, *77*, 1883–1890.

(31) Renner, T. A.; Kucera, G. H.; Blander, M. *J. Chem. Phys.* **1977**, *66*, 177.

phase is present before measuring the sample. A highly polished stainless steel mirror inside the sample cell was mounted on an externally translatable shaft that allowed the path length to be adjusted from 0 to 8750 μm while the system was under pressure. This internally mounted mirror reflected the incident beam back through the IR window to the detector.

Experimental methods were developed to obtain reliable spectra from the present reflectance cell arrangement. Since a primary reflection from the first surface of the IR window cannot be isolated optically from the reflection from the mirror within the IR cell, a subtraction method was used to remove the unwanted reflection component from the sample spectrum.²⁴

Fluid pressure was monitored to ± 1 bar with an electronic transducer (Precise Sensors, Inc., No. C451) which was calibrated against a Bourdon-tube-type pressure gauge (Heise ± 0.3 bar accuracy). The temperature of the IR reflectance cell was controlled using a three-mode controller with a platinum resistance probe (Omega, No. N2001). The temperature was also monitored with a platinum resistive thermometer (Fluka, No. 2108A). For the temperature studies, the three-mode controller was used to rapidly ramp the temperature to a new set point (approximately 10 min), and then the cell was allowed to "soak" for 20 min so that all contents and components were at the desired setpoint. The thermal equilibration of the contents could be verified by monitoring any pressure changes of the closed system. With the cell isolated from the pump by a closed valve, the pressure of a thermally equilibrated, leak-free cell remained within $\pm 1\%$ for several hours.

The sample preparation procedure was as follows. Ethane or CO₂ at 3 to 6 bar was used to purge air from the sample cell prior to introduction of the sample. Known quantities of the methyl alcohol-*d* were introduced into the IR cell. The system was then filled with ethane, CO₂, or heptane to the desired pressure using a high-pressure syringe pump (Varian 8500). The contents of the view cell were vigorously stirred with a magnetic stir bar for 15 min prior to each measurement.

To determine partial molar enthalpies, $\Delta \bar{h}_{\text{H-bond}}$, and partial molar volumes, $\Delta \bar{V}$, from changes in the equilibrium between monomers and oligomers at constant overall mole fraction of the methyl alcohol-*d*, the experiment was performed by starting with the highest density solution and then discharging small amounts of the solution to obtain progressively lower pressures or higher temperatures. Through this technique the overall mole fraction of the alcohol remained constant. The arrangement for fluid introduction and the location of the pressure transducer are shown in Figure 1. The solution was carefully discharged through a metering valve which was diffusively isolated from the cell by a 3 m long piece of 500- μm i.d. by 1.5-mm o.d. tubing so as to avoid any discrimination in the valve which would change the overall mole fraction of the solution. The amount of solvent (either carbon dioxide, ethane, or heptane) for any condition of temperature and pressure could be measured within $\pm 5\%$ (after calibration) by integration of vibrational bands for each component. The specific absorbance of these solvent bands (three combination bands near 5000 cm^{-1} for CO₂ and bands near 4300 cm^{-1} for ethane) was determined from the known path length and from the density of the pure solvents given in published data for carbon dioxide³³ and ethane,³⁴ as well as from measurements of heptane density made using an oscillating tube type of densimeter. For the Kirkwood-Bauer-Magat (KBM) plot, the values of the refractive indices for carbon dioxide and for ethane were obtained from published data for the pure fluids.³⁵

The concentration of alcohol monomer in solution was measured by first determining the specific absorbance of the monomer species at a given temperature and pressure. In dilute solutions (typically, alcohol mole fractions, $x_{\text{MeOD}} < 5 \times 10^{-3}$), methyl alcohol-*d* was found only in the monomeric, non-hydrogen-bonded form. In this dilute region, the specific absorbance was found to follow a Beer-Lambert-type of relationship with changes in alcohol concentration. The specific absorbance of the alcohol monomer was determined at each pressure studied. For the ethane and heptane solutions there was little or no change in the intensity of the ν_{1}^{OD} band with pressure. However, there was a significant change in the intensity of the ν_{1}^{OD} band in carbon dioxide solutions. Hence it was important to determine the specific absorbance of the monomer at each pressure in order to determine the monomer concentration in the more concentrated solutions where significant hydrogen bonding occurs.

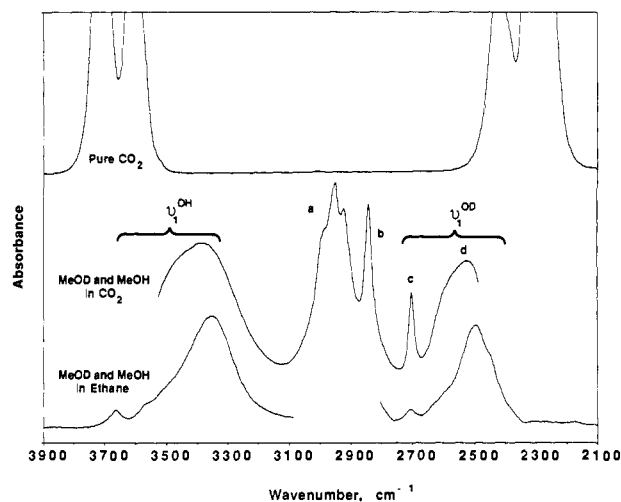


Figure 2. O-D and O-H stretching regions of an equimolar mixture of methyl alcohol and methyl alcohol-*d* in both carbon dioxide and ethane. CO₂ solvent bands interfere with the monomer band, ν_{1}^{OH} , and with ν_{1}^{OD} of the higher oligomers of the methyl alcohol-*d*. Peak assignments for methyl alcohol-*d* are as follows: C-H combination bands (a); the C-H symmetric stretch (b); the O-D stretch (ν_{1}^{OD}) of the methyl alcohol-*d* monomer (c); and the O-D stretch (also ν_{1}^{OD}) of hydrogen-bonded alcohol (d). Hydrogen bonding shifts the O-D stretch from ~ 2700 to ~ 2500 cm^{-1} . For CO₂, the $x_{\text{MeOD}} = x_{\text{MeOH}} = 0.04$, whereas for ethane, the $x_{\text{MeOD}} = x_{\text{MeOH}} = 0.01$. In both cases the pressure was 200 bar and the temperature was 40 °C. All alcohol spectra were obtained by spectral subtraction of pure solvent.

The interference of a pair of overtone and combination bands of carbon dioxide (at ~ 3600 and 3750 cm^{-1}) with the O-H stretch ($\nu_{1}^{\text{OH}} = 3682$ cm^{-1}) of the non-hydrogen-bonded alcohol required using deuterated methyl alcohol over the normal alcohol in this study. Figure 2 shows the spectra of a CO₂ solution containing both the normal and deuterated alcohol. The ν_{1}^{OH} band of the normal alcohol is obscured by a CO₂ solvent peak, whereas there is a good solvent window for the ν_{1}^{OD} band of methyl alcohol-*d*. Methyl alcohol-*d* shows a single, well-resolved peak at ~ 2700 cm^{-1} due to the free monomer (peak "c" in Figure 2) and a broad peak centered at ~ 2550 cm^{-1} (peak "d") due to the various hydrogen-bonded species (dimers, trimers, tetramers, and higher oligomers). Another CO₂ band, ν_3 , partially obscures the right tail of the ν_{1}^{OD} band (peak "d") of the intermolecular hydrogen-bonded alcohol species. The lower spectrum in Figure 2 shows a 50:50 mole mixture of MeOD and MeOH in ethane. For ethane, there are no interfering solvent bands in either the ν_{1}^{OH} or the ν_{1}^{OD} regions. The band shapes and intensities for the ν_{1}^{OD} region of methyl alcohol-*d* in ethane are remarkably similar to the ν_{1}^{OH} region (these are, of course, isotopically mixed aggregates). Although we used the deuterated alcohol for these studies, the spectra of the two alcohol isotopes in ethane show the equivalence of the ν_{1}^{OD} and ν_{1}^{OH} bands.

The hydrogen-bonding properties of the deuterated alcohol in supercritical fluids should not differ greatly from those of the normal alcohol. We know of no previous studies of deuterated alcohols in supercritical fluids, but the measured physical properties of these two isotopes show little difference. We determined the dew point pressure of a 0.03 mole fraction solution of the alcohol in carbon dioxide at 40 °C and found a pressure of 79.1 ± 1.0 bar for methyl alcohol and 78.9 ± 1.0 bar for methyl alcohol-*d*. Recently reported values³⁶ for the isotopic effect on the enthalpy of hydrogen bonding in the liquid phase are -2.70 ± 0.02 kcal/mol for methyl alcohol and -2.72 ± 0.02 kcal/mol for methyl alcohol-*d*. The difference in the thermodynamic behavior between the normal and deuterated forms of the alcohol in supercritical fluids is expected to be small. Similarly, the size distribution of intermolecularly hydrogen-bonded species is not expected to be significantly different between normal and deuterated forms of the alcohol.

Results and Discussion

Infrared Spectra. Increasing the mole fraction of the methyl alcohol-*d* increases the amount of hydrogen bonding in the solution. As shown in Figure 3, with increasing mole fraction of methyl alcohol-*d* in CO₂ the peak at ~ 2550 cm^{-1} , which is due to ν_{1}^{OD}

(32) Gurdial, G. S.; Foster, N. R.; Yun, J. S. L. In *Proceedings of the 2nd International Symposium on Supercritical Fluids*; McHugh, M. A., Ed.; Johns Hopkins University: Baltimore, MD, 1991; pp 66-69.

(33) *Gas Encyclopaedia*; Elsevier: New York, 1976.

(34) Younglove, B. A.; Ely, J. F. *J. Phys. Chem. Ref. Data* **1987**, *16*, 577-798.

(35) Besserer, G. J.; Robinson, D. B. *J. Chem. Eng. Data* **1973**, *18*, 137-140.

(36) Edwards, H. G. M.; Farwell, D. W. *J. Mol. Struct.* **1990**, *220*, 217-226.

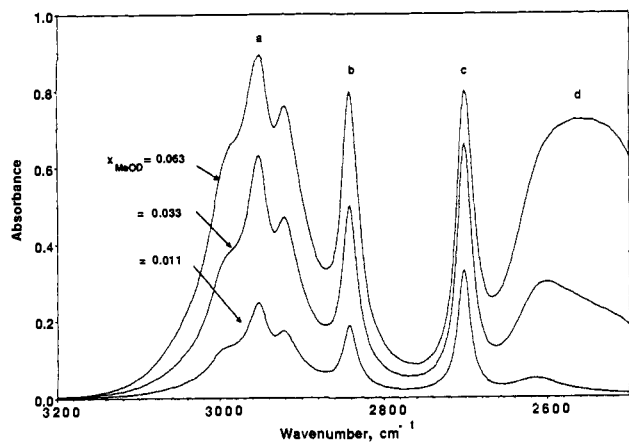


Figure 3. The C-H combination bands (a), the C-H symmetric stretch (b), and the O-D stretch of the methyl alcohol-*d* monomer (c) in carbon dioxide at 400 bar and 40 °C for three different mole fraction concentrations of the alcohol; $x_{\text{MeOD}} = 0.063, 0.033,$ and 0.011 . Hydrogen bonding shifts the O-D stretch from 2700 to 2600 cm^{-1} (d). All alcohol spectra were obtained by spectral subtraction of pure solvent.

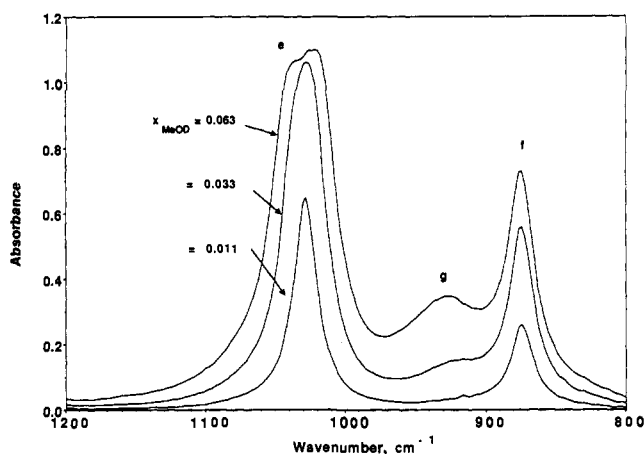


Figure 4. The O-C stretch (e) and the O-D bend (f) of methyl alcohol-*d* in carbon dioxide at 400 bar and 40 °C for three different mole fraction concentrations of the alcohol; $x_{\text{MeOD}} = 0.011, 0.033,$ and 0.063 . Hydrogen bonding shifts the O-D bend from 875 up to 925 cm^{-1} (g).

of the hydrogen-bonded alcohol, grows considerably relative to the monomeric ν_1^{OD} band at $\sim 2700 \text{ cm}^{-1}$. It is well-established in liquid-phase studies that hydrogen bonding results in a large red shift of ν_1^{OD} ³⁷ and of ν_1^{OH} .^{9,30,38} As discussed in a following section, the amount of red shift of the ν_1^{OD} band is strongly correlated to the magnitude of the solvent-solute or solute-solute interactions. The general trends of the concentration effect on the degree of intermolecular hydrogen bonding in supercritical ethane and CO_2 are similar to the effects observed in liquids. In Figure 4 we see further evidence of significant hydrogen bonding of methyl alcohol-*d* in CO_2 at higher concentrations. Figure 4 shows the OD bending vibrational band, ν_8^{OD} , of methyl alcohol-*d* in CO_2 located at 875 cm^{-1} . At higher alcohol concentrations, a peak appears at 925 cm^{-1} . We assign this 925- cm^{-1} band to ν_8^{OD} of the cyclic oligomer of the alcohol. We believe that this shift to higher energy is due to hindrance of the bending mode of the cyclic structure. With CO_2 , either the ν_8^{OD} bend at 875 cm^{-1} or the ν_1^{OD} stretch at 2700 cm^{-1} can be used to determine the amount of monomer at high total concentrations of the alcohol. The monomer concentration measured using ν_1^{OD} agrees within $\pm 5\%$ of the concentration measured using ν_8^{OD} .

The spectral data of Figures 3 and 4 are summarized in Figure 5, which shows the concentration of the monomer for various total

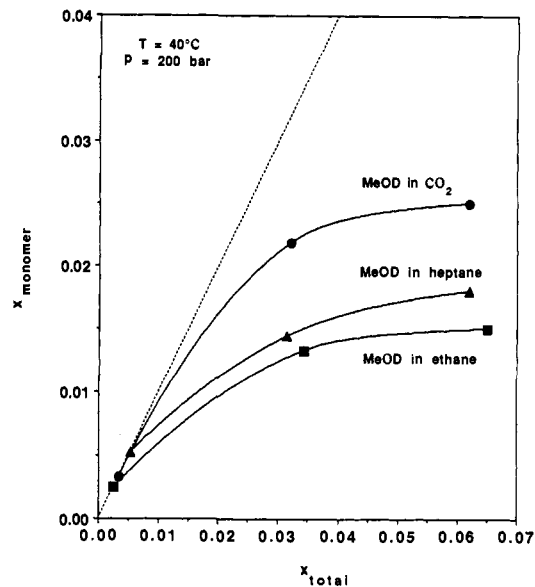


Figure 5. Concentration of monomeric methyl alcohol-*d*, x_{monomer} , for various total mole fractions, x_{total} , of the alcohol in CO_2 , ethane, and heptane at 200 bar and 40 °C.

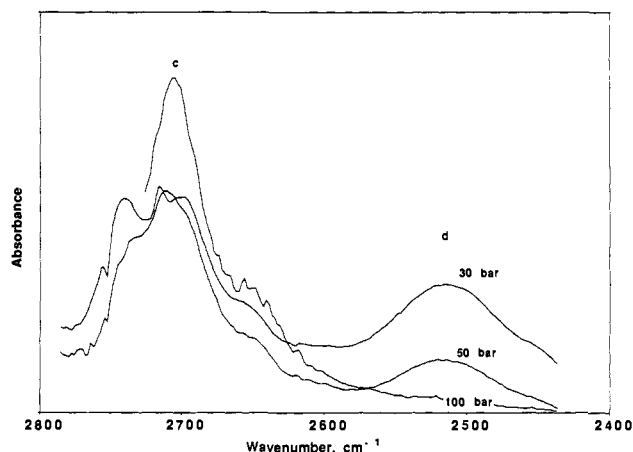


Figure 6. The effect of low fluid densities on the degree of hydrogen bonding of methyl alcohol-*d* in ethane at 40 °C and 30, 50, and 100 bar. Peak "c" is due to ν_1^{OD} of the alcohol monomer and peak "d", which is due to the hydrogen-bonded ν_1^{OD} , increases at low densities. For this experiment the molar concentration was held constant at $[\text{MeOD}] = 2.5 \times 10^{-2} \text{ M}$ for all three pressures. The corresponding mole fractions of alcohol are $x_{\text{MeOD}} = 0.018, 0.0096,$ and 0.0017 for the 30, 50, and 100 bar spectra, respectively.

mole fractions of the alcohol at 200 bar and 40 °C. Figure 5 also shows the monomer concentration for methyl alcohol-*d* in ethane and heptane. The dashed line in Figure 5 represents the case where all added alcohol is in the monomer form, i.e., no aggregation. Deviations from this line are due to intermolecular hydrogen bonding. Below a total alcohol concentration of about 0.005 mole fraction, only the monomeric form exists. Upon increasing the alcohol concentration, increasing amounts of hydrogen-bonded species are formed. It is interesting to note that of the three different solvents the amount of monomer is the lowest for ethane and the highest for CO_2 when $x_{\text{MeOD}} > 0.01$. In a related study,³⁹ we have shown that dodecanol monomer is more soluble in heptane than ethane simply because heptane, a much more polarizable solvent, can better solvate the large dipole associated with the O-H group. We see in Figure 5 the same effect of higher methyl alcohol-*d* monomer solubility in heptane compared to supercritical ethane. Surprisingly, the alcohol monomer is much more soluble

(37) Fletcher, A. N. *J. Phys. Chem.* **1972**, *76*, 2562-2571.

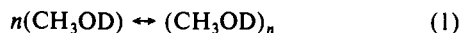
(38) Herndon, W. C.; Vincenti, S. P. *J. Am. Chem. Soc.* **1983**, *105*, 6174-6175.

(39) Fulton, J. L.; Yee, G. G.; Smith, R. D. *J. Supercritical Fluids* **1990**, *3*, 169-174.

in CO₂ than in liquid heptane; this effect cannot be explained based on the solvent dielectric constant (a simple measure of solvent strength) since the dielectric constant of CO₂ is much less than that of either ethane or heptane (1.46, 1.56, 1.92, respectively), under these conditions. The high solubility of the alcohol monomer in CO₂ constitutes tentative evidence for a weak chemical interaction between these two molecules.

In Figure 6 we see the effect of low densities of supercritical ethane on the hydrogen-bonding equilibria of the reaction. As the density is reduced, the onset of hydrogen bonding is pushed to lower and lower concentrations. An extensive amount of intermolecular hydrogen bonding occurs at 30 bar for a molar concentration of 2.5×10^{-2} M ($x_{\text{MeOD}} = 6 \times 10^{-3}$). In comparison, for heptane appreciable aggregation does not occur until the molar concentration is above 7.5×10^{-2} M ($x_{\text{MeOD}} = 1.5 \times 10^{-2}$). The large changes in the equilibrium shown in Figure 6 are mainly caused by the effect of the high isothermal compressibility of the solvent around the critical point. This experiment was conducted at constant methyl alcohol molarity utilizing an experimental technique in which the pressure of the system was increased by the addition of pure solvent. Such additions greatly shift the equilibrium of the reaction toward the monomer mainly because the mole fraction of alcohol decreases with addition of pure ethane. For experiments conducted at constant mole fraction these equilibrium changes are much less pronounced.

Enthalpy and Volume Changes for Hydrogen Bonding. The formation of intermolecularly hydrogen-bonded methyl alcohol follows a mass action model of aggregation. At low concentrations the alcohol exists only as free monomer. Upon increasing the alcohol concentration, aggregation proceeds through dimer, trimer, and finally to higher oligomers. Because of certain structural features, the methyl alcohol dimeric and especially the tetrameric species have a special stability. One expects then that, above a certain concentration of the alcohol, further additions of alcohol are likely to form mainly the tetrameric aggregate. A representation of the reaction of monomeric species to form an aggregate is:



In a solution of an alcohol in an apolar solvent, one finds a relatively narrow distribution of oligomers ($n = 2, 3, 4, 5$, and 6) which is centered around approximately $n = 4$.⁴⁰

The temperature and pressure derivatives of the equilibrium constant, K , give information on the thermodynamics of this aggregation process.

$$K = (x_{n\text{-mer}} / (x_{\text{monomer}})^n) \quad (2)$$

From a van't Hoff type relationship shown in eq 3, the partial molar enthalpy of formation, $\Delta \bar{h}_{\text{H-bond}} = \bar{h}_{n\text{-mer}} - n\bar{h}_{\text{monomer}}$, can be obtained for the aggregation process in eq 1.

$$(\partial \ln K / \partial T)_{P,n} = -(\Delta \bar{h}_{\text{H-bond}} / RT^2) \quad (3)$$

The difference between $\Delta H_{\text{H-bond}}$ of the ideal gas standard state enthalpy and the concentration and density dependent, $\Delta \bar{h}_{\text{H-bond}}$, is due to the solvation effects on the enthalpy of reaction. As an approximation in using eq 3, we assume that only two species predominate, the monomer and the cyclic tetramer. This assumption is supported by experimental and theoretical studies that show a special stability for the tetramer species (see Introduction). We also apply this equation to a solution containing a relatively high proportion of alcohol, $x_{\text{MeOD}} = 0.072$, in order to push the equilibrium toward formation of the tetrameric species. Because of the relatively high proportion of alcohol, this solution is not supercritical. Figure 7 shows the van't Hoff plots for methyl alcohol in CO₂, ethane, and heptane at a pressure of 200 bar using the monomer-tetramer model. The calculated enthalpies per hydrogen bond are given in Table I. Assuming only trimer or pentameric species in equilibrium with the monomer, we have also calculated (Table I) the enthalpy of the reaction.

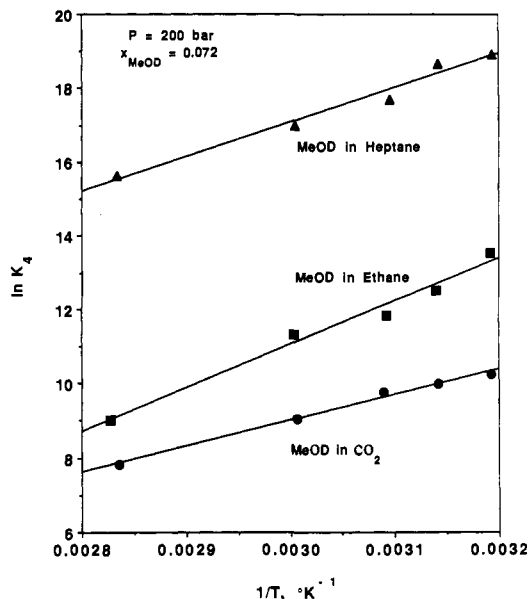


Figure 7. van't Hoff plot for the monomer-tetramer model of intermolecular hydrogen bonding of methyl alcohol-*d* in CO₂, ethane, and heptane at 200 bar with $x_{\text{MeOD}} = 0.072$. The lines represent the linearly regressed fits of the data.

Table I. Change in the Partial Molar Enthalpy of Hydrogen Bonding for Methyl Alcohol-*d* in CO₂, Ethane, and Heptane for a $x_{\text{MeOD}} = 0.065$ and a Pressure of 200 Bar According to Three Different Models of Association To Form Trimers, Tetramers, or Pentamers

solvent	$\Delta \bar{h}_{\text{H-bond}}$ per hydrogen bond, kcal/mol		
	trimer	tetramer ^a	pentamer
carbon dioxide	-3.3	-3.5 (0.3)	-3.7
ethane	-5.7	-5.9 (0.9)	-6.0
heptane		-4.7 (0.4)	

^a Values in parentheses are two standard deviations.

Measurements of the enthalpy of hydrogen bonding for the methyl alcohol dimer in the gas phase range from -2.9 to -3.5 kcal/mol.¹¹ Because of the higher stability of the tetramer, the energy per hydrogen bond is actually higher for the tetramer species than for the dimer. Renner et al.³¹ report experimentally measured enthalpies per hydrogen bond of the tetramer as -6.0 kcal/mol in the gas phase. Ab initio calculations by Curtiss et al.¹¹ give -3.7 and -7.4 kcal/mol per hydrogen bond for the linear dimer and the cyclic tetramer, respectively. The measured values of the partial molar hydrogen bond enthalpies in the three different solvents (Table I) are similar to the estimated gas-phase values. The values in Table I include any solvent interaction effects on the hydrogen-bonding enthalpy since the molecular densities in all cases studied are far from the gas-phase limits. At these conditions, ethane has a much lower dielectric constant than that of heptane, and, of these two solvents, ethane would be most similar to the gas-phase values for the tetrameric species. The measured $\Delta \bar{h}_{\text{H-bond}}$ value for ethane of -5.9 kcal/mol per hydrogen bond is only slightly lower than the reported gas-phase values. The measured values of the hydrogen bond energy in heptane are about 1 kcal/mol smaller than for ethane. This is likely owing to the stronger interaction of the solvent with the monomeric species. Although we are using the deuterated form of the alcohol rather than the normal alcohol, the isotopic effect on the energy of hydrogen bonding is expected to be small based on the small differences in the dew point values of the two isotopes.

The change in the partial molar enthalpy for hydrogen bonding in CO₂ is smaller than that for either ethane or heptane even though the dielectric constant of CO₂ is lower than that of either alkane. One would expect $\Delta \bar{h}_{\text{H-bond}}$ for CO₂ to be even closer to the gas-phase value than ethane. These results however suggest

(40) Bartczak, W. M. *Ber. Bunsenges. Phys. Chem.* 1979, 83, 987-992.

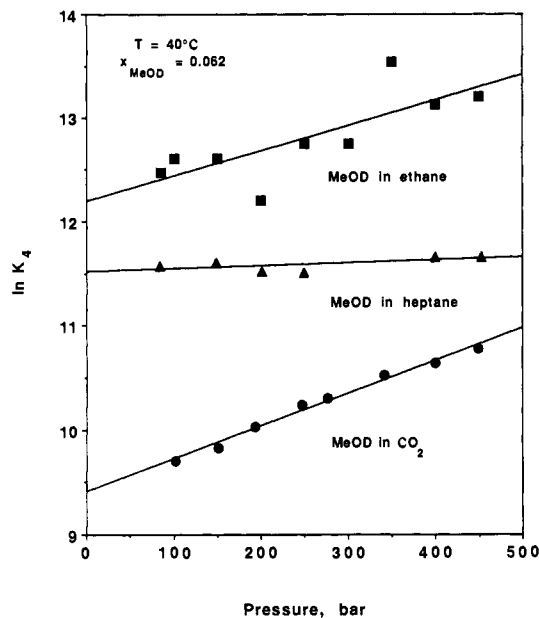


Figure 8. The effect of pressure on the chemical equilibria (monomer-tetramer model) of intermolecular hydrogen bonding of methyl alcohol-*d* in CO₂, ethane, and heptane at 40 °C with $x_{\text{MeOD}} = 0.062$. The lines represent the linearly regressed fits of the data.

a strong interaction between CO₂ and the monomer alcohol having an interaction energy of a few kilocalories/mole. The derivative, $\partial \ln K_4 / \partial(1/T)$, for CO₂ is fairly linear over the temperature range shown in Figure 7 because at 200 bar and 40 °C the fluid is far enough away from the critical point to avoid large nonlinearities observed by others²³ near the critical region. For this solution, where $x_{\text{MeOD}} = 0.072$ the system is below its critical temperature ($T_c = 50$ °C, $P_c = 95$ bar).³² Because the stoichiometry of the association of CO₂ with the alcohol monomer is not known, the number of possible interactions per CO₂ molecule is not known. The lowering in the enthalpy of formation may be caused by two or three CO₂'s interacting with the monomer, or perhaps tens to hundreds of molecules. These results confirm previous reports from gas-phase studies of the CO₂/methyl alcohol system⁴¹ which have also shown some type of weak chemical association between these two molecules.

The pressure derivative of the equilibrium constant shown in eq 4 gives the change in the partial molar volume, $\Delta \bar{V}$, for the

$$-RT(\partial \ln K / \partial P)_{T,x} = \Delta \bar{V} \quad (4)$$

reaction to form the hydrogen-bonded species from the free monomer. In this case $\Delta \bar{V}$ represents the partial molar volume change under the same conditions as K and not at infinite dilution.

In eq 4, the equilibrium constant, K , is in units of mole fraction. For K to be expressed in molarity, an additional isothermal compressibility term must be added to eq 4.⁴² There is an appreciable difference in the equilibrium of the reaction if the experiment is conducted at constant molar concentration rather than constant mole fraction. For the constant molarity experiment there is a much more pronounced shift of the equilibrium toward the monomer at higher pressures. This is due to a much larger effect of the isothermal compressibility on the equilibrium⁴² when the experiment is conducted in the constant molarity mode. Because the objective of this experiment was primarily to obtain values for $\Delta \bar{V}$, it was undesirable to have to account for the large isothermal compressibility term especially when its value must be independently measured for these more concentrated solutions. Hence, by conducting the experiment at constant mole fraction, the effect of the isothermal compressibility on the change of the equilibrium could be reduced.

Table II. Change in the Partial Molar Volumes, $\Delta \bar{V}$, for Hydrogen Bonding of Methyl Alcohol-*d* in CO₂, Ethane, and Heptane at 40 °C for Two Concentrations of the Alcohol, $x_{\text{MeOD}} = 0.062$ and 0.031

solvent	x_{MeOD}	$\Delta \bar{V}_{\text{H-bond}}, \text{cm}^3/\text{mol}$		
		trimer	tetramer ^a	pentamer
carbon dioxide	0.062	-62.3	-79.2 (6.9)	-96.2
ethane	0.062	-47.8	-62.2 (38.6)	-76.8
heptane	0.062		-6.9 (8.8)	
carbon dioxide	0.031	-54.8	-65.9 (10.7)	-76.9
ethane	0.031	-32.9	-42.3 (30.4)	-51.5
heptane	0.031		-13.7 (9.4)	

^a Values in parentheses are two standard deviations.

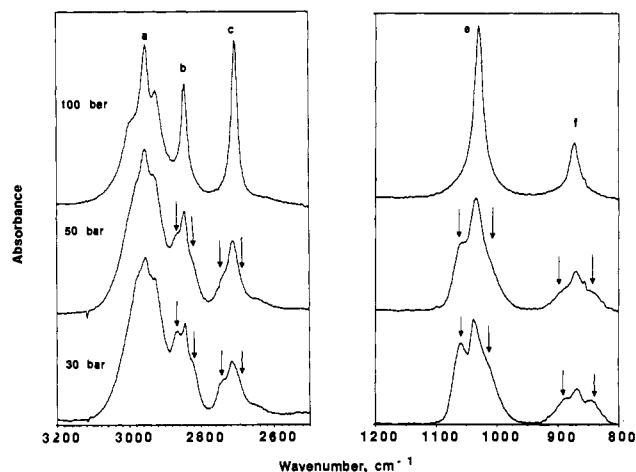


Figure 9. The rotational-vibrational bands for densities near and below the critical density showing the evolution of the P and R branches of the various vibrational modes of methyl alcohol-*d* in CO₂ as the density is decreased. The molar concentration of alcohol is $[\text{MeOD}] = 2.2 \times 10^{-2}$ ($x_{\text{MeOD}} \sim 5 \times 10^{-3}$).

Figure 8 shows the effect of pressure on the chemical equilibria at constant alcohol mole fraction. As expected, the effect of pressure on the equilibria results in a moderate change in $\Delta \bar{V}$ in ethane and CO₂ with little or no change in liquid heptane. In Table II, the $\Delta \bar{V}$ data for two different concentrations is presented with their corresponding fits to three simple models of hydrogen bonding: monomer-trimer, monomer-tetramer, and monomer-pentamer. The experiments were conducted relatively far away from the critical point where only minor effects of the fluid compressibility on the partial molar volume are observed. The CO₂ data at 100 bar are perhaps the closest to a critical point, although no deviations from linearity were observed. This is because at $x_{\text{MeOD}} = 0.062$ the system is approximately 5° below its critical temperature ($T_c = 45$ °C, $P_c = 88$ bar).³² The value reported for methyl alcohol-*d* in heptane in Table II is similar to the approximate value of $-4.6 \text{ cm}^3/\text{mol}$ reported for *n*-butyl alcohol in 2,3-dimethylbutane.⁴³ The larger $\Delta \bar{V}$ for ethane and CO₂ is partially caused by the contraction of solute volume associated with the transition from approximately four monomer molecules to a single intermolecularly hydrogen-bonded aggregate; this value may also involve contributions due to increased clustering of the solvent around the larger aggregate.

Rotational-Vibrational Bands. Figure 9 shows the solvent-subtracted spectra of methyl alcohol-*d* in CO₂ for pressures near and below the critical pressure. At pressures below 100 bar there is a significant amount of broadening of all of the vibrational bands within the 700- to 3500-cm⁻¹ region. Singly resolved peaks show evolution to triplets at low densities due to increasing rotational freedom of the alcohol. The peak forming to the right of the main vibrational band is the coupled rotation-vibration R branch, and the peak forming to the left is the P branch. Figure 9 shows the splitting of methyl alcohol-*d* peaks to R and P branches for (i) ν_8^{OD} , the O-D bend at 875 cm⁻¹; (ii) ν_4^{CO} , the C-O stretch at 1035

(41) Hemmaphardh, B.; King, A. D. *J. Phys. Chem.* **1972**, *76*, 2170-2175.

(42) Isaacs, N. S. *Liquid Phase High Pressure Chemistry*, John Wiley: New York, 1981.

(43) Fishman, E.; Drickamer, H. G. *J. Chem. Phys.* **1956**, *24*, 548-533.

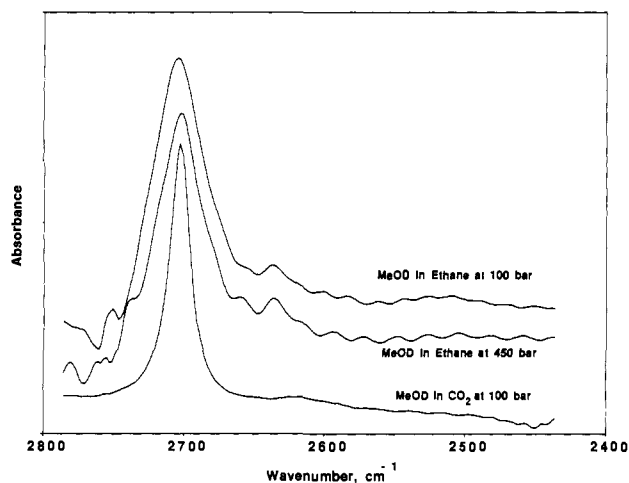


Figure 10. Comparison of the monomer O–D stretch of methyl alcohol-*d* in ethane at 100 and 450 bar and in carbon dioxide at 100 bar. Narrowing of peaks in CO₂ at 100 bar and in ethane at 450 bar indicates loss of rotational freedom. In all cases $T = 40\text{ }^{\circ}\text{C}$ and $\chi_{\text{MeOD}} = 0.003$.

cm⁻¹; (iii) ν_1^{OD} , the O–D stretch at 2700 cm⁻¹; and (iv) ν_2^{CH} , the C–H stretch at 2850 cm⁻¹. The other C–H stretch and combination bands around 2980 cm⁻¹ show evidence of rotational broadening but are unresolved because of the overlap of multiple vibrational bands. The region near the critical point of the solvent could not be investigated in more detail in the other studies since the monomer peak is complicated by the enhanced rotational freedom.

Figure 10 shows ν_1^{OD} of the alcohol monomer in CO₂ and ethane. At 100 bar, the ν_1^{OD} peak in CO₂ is significantly narrower than in ethane, having a full width at half-maximum (fwhm) of 20.6 cm⁻¹ in CO₂ and a fwhm of 42.6 cm⁻¹ in ethane. Although the molecular densities of ethane and CO₂ are similar under these conditions, the broader ethane peak suggests greater rotational freedom in ethane. The ν_1^{OD} monomer peak narrows slightly in ethane from 42.6- to 38.7-cm⁻¹ fwhm when the pressure is increased from 100 to 450 bar, suggesting significant rotational freedom even at 450 bar. Recently Conrad et al.²⁷ reported IR evidence of nearly free rotation of water and methyl alcohol in weakly interacting solvents such as liquid alkanes and were able to satisfactorily describe the broadening by a rotational diffusion model with free rotation time of about 0.1 ps. At 450 bar, the density of supercritical ethane approaches liquid-like densities. Since ethane is a more weakly interacting solvent than the higher alkanes, one would expect greater rotational freedom.

The restriction of rotational freedom of a solute in a supercritical fluid as the fluid density increases should appreciably affect the internal energy of that solute. However, the relationship between the degree of rotational broadening of a vibrational peak and the actual restriction of rotational states cannot be directly determined. A quantum mechanical fit such as the one used by Conrad et al.²⁷ may be required. A significant change in the amount of rotational energy of a solute in a supercritical fluid solution would be an important term in the total energy of the system, especially near the critical point where the large changes in the rotation-vibration bands were observed.

Interaction of Carbon Dioxide with Methyl Alcohol-*d*. The IR spectra strongly suggest the existence of a specific interaction between CO₂ and methyl alcohol. There are five different indicators of such an interaction: (1) the alcohol intermolecular hydrogen-bonding equilibria are perturbed, (2) the measured enthalpy of hydrogen bonding is lower, (3) the alcohol shows less rotational freedom, and (4) the ν_1^{OD} band position and (5) intensity show behavior which is characteristic of interacting solvents. Whether this interaction is described as a weak chemical effect or simply an electrostatic effect, its source is likely the attraction between the relatively large quadrupole on the CO₂ and the large dipole of the alcohol group. We can speculate that a weak complex forms between one or two CO₂ molecules with a methyl alcohol

molecule, although there is no direct evidence for such a structure from this study.

As shown in Figure 5, the equilibria between the alcohol monomer and hydrogen-bonded species are significantly different for CO₂ than for a "noninteracting" solvent such as ethane. In CO₂ much more of the alcohol is in the monomer form than in ethane. This is opposite to what one would expect based on the molecular polarizabilities of the solvents at the molecular densities used in this study. Because of a weak chemical interaction between CO₂ and the alcohol, as represented in eq 5, the equilibrium is



shifted toward the non-hydrogen bonded form of the alcohol. Further, the measured enthalpy (Table I) for hydrogen bonding is significantly lower than for "noninteracting" alkanes solvents. The enthalpy data suggest that the energy of interaction of the CO₂ with the alcohol monomer is on the order of 1–2 kcal/mol of alcohol. Because the number of CO₂ molecules that interact with a single alcohol has not been determined, the energy of interaction could involve tens and possibly hundreds of CO₂ molecules, and thereby proportionally reduce the interaction per CO₂ molecule. If this contribution arises from dipole–quadrupole interactions (potential energy $\sim r^{-8}$), then the interactions are shorter range⁴⁴ than the dispersion forces ($\sim r^{-6}$) which would suggest a smaller cluster size. This hypothesis is supported by the measurements of $\Delta\bar{V}$ which show approximately the same value of $\Delta\bar{V}$ for CO₂ as that found for ethane where there are no dipole–quadrupole interactions. Alcohol in the tetrameric form is not capable of the same dipole/quadrupole interactions because hydrogen bonding significantly reduces the magnitude of the alcohol dipole. Hence one would expect a more positive value of $\Delta\bar{V}$ than that found for ethane if large clusters were forming around the methyl alcohol monomers. However, little difference in $\Delta\bar{V}$ values is observed. Thus we believe a complex involving only a few CO₂ molecules with the alcohol monomer is most likely.

Figure 10 shows that the degree of rotation of methyl alcohol-*d* is significantly less in CO₂ than in ethane. Formation of a CO₂ cluster or complex with the alcohol monomer as represented by eq 5 would either lead to a loss of rotational freedom through collisional hindrance or significantly change the rotational energy states by formation of a complex having different rotational energy levels. This lack of rotational structure in the CO₂ spectra is further evidence of an interaction with the alcohol. Chialvo et al.²⁸ have shown a pronounced effect of the quadrupole of a CO₂-like molecule, simulated by molecular dynamics, on the slowing down of its rotational dynamics. The larger dipole–quadrupole interactions of methyl alcohol/CO₂ should greatly restrain the rotational freedom of the alcohol.

A solvatochromic shift of a vibrational band of a solute is observed as the dielectric constant of the solvent is changed. The magnitude of these shifts can be related through the semiempirical relationship of the Kirkwood–Bauer–Magat (KBM) model, given as

$$\left(\frac{\nu_g - \nu_l}{\nu_g}\right) = k \left(\frac{\epsilon - 1}{2\epsilon + 1}\right) \quad (6)$$

where ν_g and ν_l are the locations of the vibrational peaks in the gas phase and in the liquid or solvent phase, respectively. The functionality for the dielectric constant, ϵ , shown on the right-hand side of eq 6 is directly related through some proportionality constant, k , to the observed solvatochromic shifts of the peak. The validity of this relationship for ν_1^{OH} of water has been established.^{27,45} "Noninteracting" solvents such as the alkanes and fluorocarbons show a linear relationship between the KBM function and the shift of the ν_1^{OH} peak. These solvents interact only through their induced dipole with the dipole or induced dipole

(44) Prausnitz, J. M. *Molecular Thermodynamics of Fluid-Phase Equilibria*; Prentice-Hall: Englewood Cliffs, NJ, 1969.

(45) Scherer, J. R. In *Advances in Infrared and Raman Spectroscopy*; Clark, R. J. H., Hester, R. E., Eds.; Heyden & Sons: Philadelphia, PA, 1978; pp 149–216.

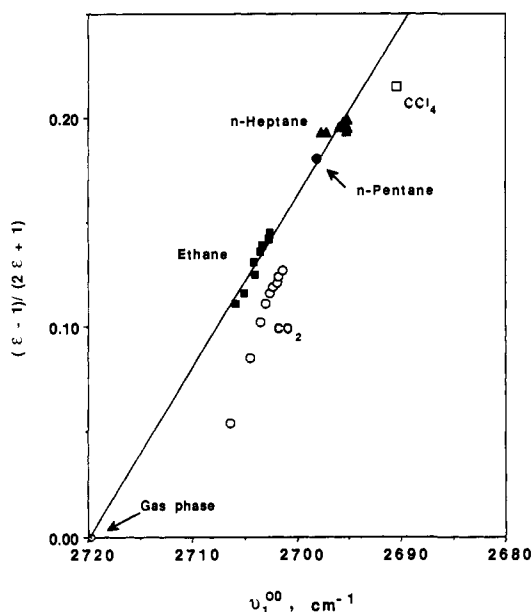


Figure 11. KBM plot of ν_1^{OD} for methyl alcohol-*d* in CO_2 , ethane, and heptane at 40 °C. Values for CO_2 deviate from linear relationship of the noninteracting alkane solvents. Ethane, heptane, and CO_2 values represent a range of pressures from 85 to 450 bars, whereas the pentane and CCl_4 values are at 1 bar. In all cases $T = 40$ °C and $x_{\text{MeOD}} = 0.003$.

of the alcohol molecules. Solvents having any type of weak chemical interaction with the O-H group deviate from the KBM relationship with larger than expected red shifts. Examples of solvents showing significant deviation are the alkenes, benzene, and CCl_4 .

A KBM plot for ν_1^{OD} of methyl alcohol-*d* in various liquid and supercritical solvents is shown in Figure 11. The alkanes, supercritical ethane, and liquid pentane and heptane show the expected linear relationship of the band shift with the KBM function. The data points for ethane represent a range of pressures from 85 to 450 bar. As the density of supercritical ethane is increased with increasing pressure, ν_1^{OD} undergoes a red shift corresponding to an increase of the fluid dielectric constant with pressure. The red shift of ν_1^{OD} of methyl alcohol-*d* in CO_2 for a range of pressures clearly deviates from the linear relationship of the noninteracting alkanes. Again we have evidence of a specific interaction between CO_2 and methyl alcohol-*d*.

Finally we examine the ν_1^{OD} band intensity. Glew and Rath⁴⁶ have established that a linear relationship exists between the ν_1^{OH} shift of methyl alcohol and its band area. As the solvent-induced red shift increases, so does the band area of ν_1^{OH} . Strong hydrogen-bonding solvents yield a 10-fold increase in ν_1^{OH} intensity over simple van der Waals solvents.⁴⁷

In Figure 12, a plot of the band area of ν_1^{OD} versus the system pressure for the three fluids is shown. The intensity of the ν_1^{OD} is much larger in CO_2 than in the two alkane solvents, and the intensity increases as the pressure or density of the fluid increases. Both the heptane and the ethane show little or no pressure effect. For heptane this behavior was expected since these pressure ranges have little effect on the density of the solvent. However, for ethane there are appreciable changes in the fluid density, and an increase in the band area with pressure might be expected. No appreciable intensity increases were observed. The high intensity of ν_1^{OD} in CO_2 provides additional evidence of a weak chemical interaction

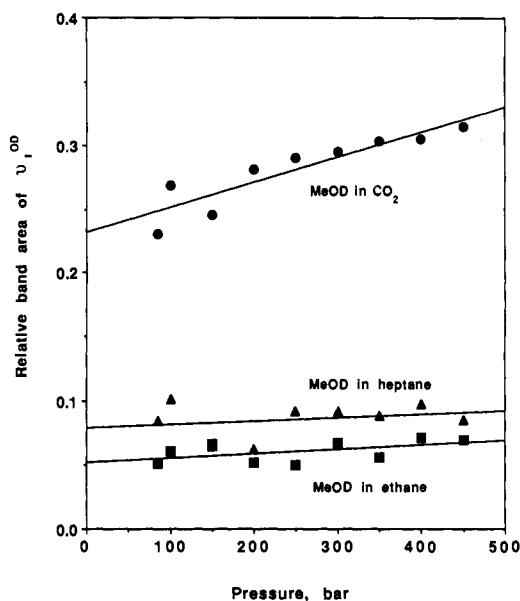


Figure 12. Relative band area of the ν_1^{OD} versus pressure for methyl alcohol-*d* in CO_2 , ethane, and heptane. In all cases $T = 40$ °C and $x_{\text{MeOD}} = 0.003$.

between CO_2 and the methyl alcohol-*d*.

Conclusions

The solvation phenomena examined in this work should provide a basis for a more appropriate treatment of hydrogen bonding in supercritical fluids. The onset of hydrogen bonding in ethane occurs at methyl alcohol concentrations above about $x_{\text{MeOD}} = 0.003$. This intermolecular hydrogen bonding becomes extensive at concentrations above about $x_{\text{MeOD}} = 0.05$ in a region where the tetramer is believed to be the dominant alcohol species. In CO_2 , the onset of hydrogen bonding occurs at a higher alcohol concentration ($x_{\text{MeOD}} = 0.005$) than expected due to a weak chemical interaction between CO_2 and methyl alcohol, which shifts the equilibria toward the monomer form of the alcohol. The IR spectral data provide further evidence of a special interaction between the alcohol monomer and CO_2 solvent, likely involving a weak complex of the alcohol and a small number of CO_2 molecules. These observations may help to explain the large deviations of the predicted excess molar enthalpies for the CO_2 -methyl alcohol mixtures.²²

The methyl alcohol monomer/aggregate equilibrium was found to be shifted toward aggregation by decreasing the temperature or by increasing the pressure (at constant mole fraction). At densities near or below the critical density of the fluid, the bands assigned to the various vibrational modes of methyl alcohol show broadening which is characteristic of increased rotational freedom. Hydrogen bonding in the region very near to the critical point could not be investigated because of the appearance of rotational-vibrational bands. Measurements of the enthalpy for hydrogen bonding showed similar values in ethane as found in the liquid alkane solvents. However, the enthalpy of hydrogen bonding for methyl alcohol in CO_2 is significantly lower at the same temperature and pressure because of the CO_2 /methyl alcohol interaction.

Acknowledgment. This research was supported by the Director, Office of Energy Research, Office of Basic Energy Sciences, Chemical Sciences Division of the U.S. Department of Energy, under Contract DE-AC06-76RLO 1830.

Registry No. MeOD, 1455-13-6; ethane, 74-84-0; CO_2 , 124-38-9.

(46) Glew, D. N.; Rath, N. S. *Can. J. Chem.* 1971, 49, 837-856.

(47) England-Kretzer, L.; Fritzsche, M.; Luck, W. A. P. *J. Mol. Struct.* 1988, 175, 277-282.